

# Imaging and spectroscopy of galaxies associated with two $z \sim 0.7$ damped Lyman- $\alpha$ absorption systems

Mark Lacy<sup>1,2,3</sup>, Robert H. Becker<sup>2,3</sup>, Lisa J. Storrie-Lombardi<sup>1</sup>, Michael D. Gregg<sup>2,3</sup>,  
Tanya Urrutia<sup>3</sup>, Richard L. White<sup>4</sup>

## ABSTRACT

We have identified galaxies near two quasars which are at the redshift of damped Lyman- $\alpha$  (DLA) systems in the UV spectra of the quasars. Both galaxies are actively forming stars. One galaxy has a luminosity close to the break in the local galaxy luminosity function,  $L^*$ , the other is significantly fainter than  $L^*$  and appears to be interacting with a nearby companion. Despite the strong selection effects favoring spectroscopic identification of the most luminous DLA galaxies, many of the spectroscopically-identified DLA galaxies in the literature are sub- $L^*$ , suggesting that the majority of the DLA population is probably sub- $L^*$ , in contrast to MgII absorbers at similar redshifts whose mean luminosity is close to  $L^*$ .

*Subject headings:* Quasars: absorption lines — galaxies: distances and redshifts — quasars: individual (FBQS J0051+0041, FBQS J1137+3907)

## 1. Introduction

Damped Ly $\alpha$  (DLA) absorbers in quasar spectra are the class of absorbers with the highest column density of neutral hydrogen ( $N_{HI} \geq 2 \times 10^{20} \text{cm}^{-2}$ ). They are important as it can be shown that they contain the bulk of the neutral hydrogen content of the Universe (e.g. Storrie-Lombardi & Wolfe 2000). The similarity of the column densities of DLAs to those through the disks of spiral galaxies have lead some authors to consider them as the direct progenitors of present-day spirals (e.g. Prochaska & Wolfe 1998). However, dwarf galaxies and low surface brightness galaxies (LSBGs) also can have similar columns (Boissier, Peroux & Pettini 2003), and metallicity arguments

support dwarf galaxies (Pettini et al. 1999). Theorists have interpreted them in the context of hierarchical galaxy formation models as sub-units which will eventually merge to form  $L^*$  galaxies today (Haehnelt, Steinmetz & Rauch 1998; Maller et al. 2001) or as dwarf galaxies in which star formation is suppressed by supernova feedback (Efstathiou 2000).

The reason for the proliferation of theories for the nature of DLAs is that reliably identifying the galaxies responsible for the absorption, even at  $z < 1$ , has proven to be very difficult. Imaging studies of  $z < 1$  absorbers, e.g. Le Brun et al. (1997); Rao et al. (2002) indicate that a range of galaxy types might be responsible for producing DLAs, but few candidate DLAs have measured redshifts, so reliable constraints on the nature of the DLA population remain poor. Paradoxically, MgII absorbers, with much lower column densities on average, have been easier to identify. They seem to be sampling the normal galaxy population, with a mean luminosity of  $\sim L^*$  at  $< z >= 0.6$  (Steidel, Dickinson & Persson 1994; Steidel et al. 2002). Possible reasons for the difficulty of identifying the galaxies causing DLA systems include small impact parameters, low stellar

<sup>1</sup>SIRTF Science Center, MS 220-6, California Institute of Technology, 1200 E. California Boulevard, Pasadena, CA 91125; mlacy@ipac.caltech.edu, lisa@ipac.caltech.edu

<sup>2</sup>IGPP, L-413, Lawrence Livermore National Laboratory, Livermore, CA 94550; bob@igpp.ucllnl.org, gregg@igpp.ucllnl.org

<sup>3</sup>Department of Physics, University of California, 1 Shields Avenue, Davis, CA 95616; urrutia@physics.ucdavis.edu

<sup>4</sup>Space Telescope Science Institute, 3700 San Martin Drive, Baltimore, MD 21218; rlw@stsci.edu

luminosities or low surface brightnesses. So far only six  $z < 1$  DLAs have been spectroscopically-confirmed (and all of these are at  $z < 0.6$ ). Several are dwarf or low surface brightness galaxies, the best-studied example of which is SBS 1543+5921 (Bowen, Tripp & Jenkins 2001), but the DLA absorber of AO 0827+24 is a fairly normal, luminous spiral (Steidel et al. 2002). Many more suggested identifications have been made on the basis of proximity to the quasar and consistent photometry, but the reliability of these is unclear.

DLAs are easy to identify in the spectra of high redshift ( $z \gtrsim 2$ ) quasars as they show up clearly in observed optical spectra, but they are hard to identify at lower redshift. By adopting the strategy of taking UV spectra with the *Hubble Space Telescope* (*HST*) of the highest rest-frame equivalent width ( $EW_0$ ) MgII absorbers in the literature, Rao & Turnshek (2001) were able to identify a sample of lower redshift ( $z \sim 0.3$ – $1.7$ ) DLAs (see also Boisse & Bergeron 1998). High  $EW_0$  MgII absorbers also typically show high  $EW_0$  FeII absorption lines, and these have been hypothesised to be better tracers of cool gas than MgII (Bergeron & Stasińska 1986). We have therefore used the FIRST Bright Quasar Survey (FBQS; White et al. 2000; Becker et al. 2001) to select a similar sample with  $EW_0$  (FeII 2600Å)  $\geq 1$ Å. We have taken spectra of 26 of the sample with STIS on the *HST* to look for DLA systems. We have followed up this sample using the Keck telescope, taking near-infrared images in sub-arcsecond seeing, medium-resolution spectra of the quasars, and low-resolution spectra of the candidate absorbers. We are mid-way through spectroscopic follow-up of the FBQS sample, and have identified four galaxies with redshifts the same as that of the FeII absorbers. Of these four, however, only two are associated with absorbers which are definitely damped. These two galaxies, near the quasars FBQS 0051+0041 (R.A. 00<sup>h</sup>51<sup>m</sup>30<sup>s</sup>.49 Dec. +00°41′49″.91 (J2000); absorber redshift,  $z_{\text{abs}} = 0.74$ ; quasar redshift,  $z_Q = 1.19$ ; apparent magnitude  $B = 18.5$ ) and FBQS 1137+3907 (R.A. 11<sup>h</sup>37<sup>m</sup>09<sup>s</sup>.46 Dec. +39°07′23″.60 (J2000);  $z_{\text{abs}} = 0.72$ ;  $z_Q = 1.02$ ;  $B = 18.4$ ), form the subject of this paper.

We assume a cosmology with  $\Omega_M = 0.3$ ,  $\Omega_\Lambda = 0.7$  and  $H_0 = 70 \text{ km s}^{-1} \text{ Mpc}^{-1}$  throughout. Where we have referenced galaxy luminosities,  $L$ , to the

present-day values of the break in the luminosity function,  $L^*$  we have used  $L^*$  values of Norberg et al. (2002) in  $B$ , Lin et al. (1996) in  $R$  and Loveday (2000) in  $K$ , adjusted to our passbands and cosmology as necessary ( $M_B^* = -20.2$ ,  $M_R^* = -21.1$ ,  $M_K^* = -24.4$ ). The  $k$ -corrections have been derived using a model 5Gyr old Sd galaxy from the Pegase library (Rocca-Volmerange & Fioc 1997). We picked this model as representative of a moderately young, star-forming galaxy, a decision motivated by the discovery of [OII] emission from the candidate DLA galaxies.

## 2. Imaging Observations

FBQS 0051+0041 was imaged with the Echellette Spectrograph and Imager (ESI) on Keck-II and FBQS 1137+3907 with the Near-Infrared Camera (NIRC) on Keck-I. Details of the observations are given in Table 1. A sequence of short (3–5min) dithered exposures of each object were taken. After dark subtraction and flat-fielding with dome flats the data were analysed using DIMSUM and XDIMSUM in IRAF, respectively. The DIMSUM package performs two passes on the data. In the first pass, a background image is made from a median of the dithered frames and the data are combined with integer pixel shifts to make masks which are used to mask out objects when constructing an improved sky background image for the second pass. In the second pass, the improved background is subtracted from the images before they are shifted and coadded, and a magnification factor may be applied to the data. The pixel scale of the ESI image was sufficiently small compared to the seeing that no magnification was used in the second pass for FBQS 0051+0041. The operation of the DIMSUM package is explained in more detail in Stanford, Eisenhardt & Dickinson (1995). The XDIMSUM package is a modification of DIMSUM by L. Davis at NOAO. Amongst other improvements it runs significantly faster and allows non-integer magnification factors in the second pass. We used a factor of 2.3 for the FBQS 1137+3907 image.

Photometry for FBQS 0051+0041 was obtained using observations of the Landolt (1992) standard 107-215, and that for FBQS 1137+3907 from observations of the standard star P266-C from Persson et al. (1998). Both quasar fields were imaged in photometric conditions. The  $5\sigma$  limiting magni-

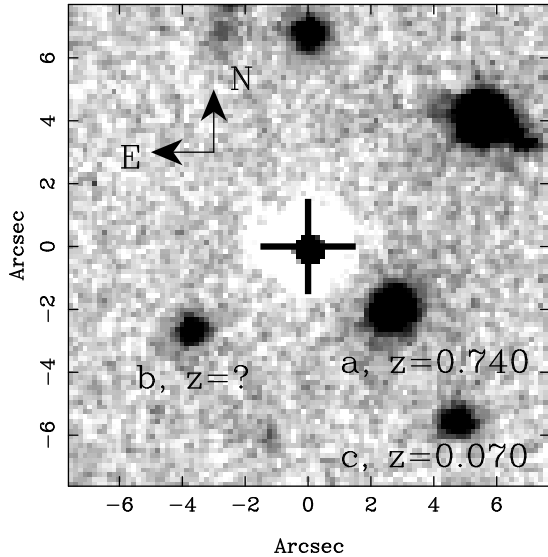


Fig. 1.— The field of FBQS 0051+0041 in  $I$ . The quasar has been partially subtracted from near the center of the image, and its position is marked with a cross. The DLA candidate is galaxy ‘a’

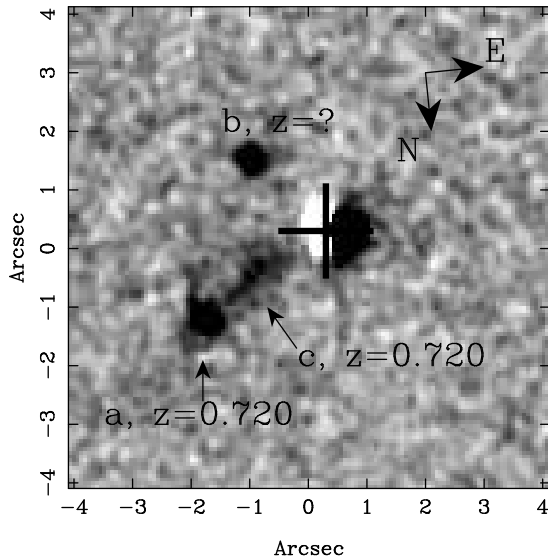


Fig. 2.— The field of FBQS 1137+3907 in  $K'$ . The quasar has been partially subtracted from near the center of the image, and its position is marked with a cross. Galaxies ‘a’ and ‘c’ are most probably associated with the DLA system.

tudes in 2-arcsec diameter apertures are  $I = 25.4$  for the FBQS 0051+0041 field and  $K' = 21.9$  for the FBQS 1137+3907 field.

We performed approximate subtractions of the quasars using point spread functions derived from either from a star in the same image (FBQS 0051+0041) or from other quasars observed on the same night (FBQS 1137+3907). The PSF was fitted with a least-squares fit using code developed for fitting quasar host galaxies (Lacy et al. 2002). The particular algorithm employed here subtracted the PSF such that the mean value within a radius  $r_{\text{in}}$  from the center of the quasar was set to zero. The values of  $r_{\text{in}}$  used were  $0''.6$  for FBQS 0051+0041 and  $0''.3$  for FBQS 1137+3907. Neither PSF subtraction was very satisfactory, as we made no serious attempt to obtain good, unsaturated PSFs for the quasars. They have successfully removed the wings of the PSFs, however. The resulting images are shown in Figures 1 and 2.

### 3. HST Spectroscopy

The quasars were observed with the STIS with the MAMA detectors and the G230L grating as part of program 9051. The  $0''.2$  slit was used, giving a spectral resolving power of 330 at the redshifted wavelength of  $\text{Ly}\alpha$ , corresponding to a velocity resolution of  $\approx 900\text{kms}^{-1}$ . Each quasar was observed for two 1100s exposures, the second exposure being dithered  $2''$  along the slit. The UV spectrum of FBQS 1137+3907 shows it to be a high-ionization broad-absorption line (BAL) quasar, with a BAL trough blueshifted by  $13000\text{kms}^{-1}$ . Fortunately, the Lyman- $\alpha$  absorption line is clear of the BAL troughs, falling just to the red of the OVI trough in the quasar spectrum. The spectra are shown in Figures 3 and 4.

A detailed discussion of the HST spectra and measurements of the damped absorbers are provided in a companion paper (Storrie-Lombardi, et. al. 2003, in preparation). The column densities of the damped absorbers were initially estimated from measurements of the equivalent widths of the absorption lines with the redshift determined from the low ionization metal lines from our ground-based spectra. Profiles were then fit iteratively to determine the best fit column density and redshift

for HI absorption feature. The column densities should be accurate to  $\pm 0.1$  and the redshifts to  $\pm 0.005$ . Though higher resolution spectra covering multiple lines in the Lyman series would be ideal for this purpose, the substantial HST time that would be involved in obtaining them makes such observations impractical for large samples of objects. At higher redshifts, we have shown via observation and simulation that moderate resolution spectra provide an excellent estimate for the measured HI column densities (e.g. Storrie-Lombardi et. al. 1996; Storrie-Lombardi & Wolfe 2000), which gives us high confidence that the features in these spectra are damped and are not blends of lower column density lines.

#### 4. Keck spectroscopy

The candidate absorbers were observed with the Low Resolution Imaging Spectrometer (LRIS) on Keck-I using the 300 line  $\text{mm}^{-1}$ , 5000Å blaze grating in the red arm and a 1-arcsecond slit (see Table 2). This combination results in a spectral resolving power of  $\approx 500$ , corresponding to a velocity resolution of  $\approx 600 \text{ km s}^{-1}$ . The wavelength range covered was from  $\approx 5000 - 10000 \text{ Å}$ .

In addition, observations of the quasars were made with ESI on Keck-II to obtain medium-resolution spectra of the absorption lines. The FeII 2586 and 2600Å lines fell in a noisy region near an order overlap in the ESI spectra, but the MgII 2796 and 2803Å lines were detected at high signal-to-noise in both quasars. FBQS 0051+0041 was observed with ESI on 2000 December 31 with a  $0''.75$  slit, and FBQS 1137+3907 on 2001 March 20 with a  $1''$  slit, yielding resolving powers of 5400 and 4100 respectively. The ESI spectra of the quasars in the region around MgII are shown in Figures 5

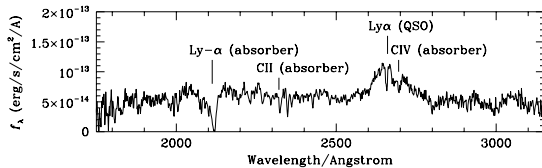


Fig. 3.— STIS spectrum of FBQS 0051+0041. The quasar ( $z_Q = 1.19$ ) and absorber ( $z_{\text{abs}} = 0.74$ ) features are labelled.

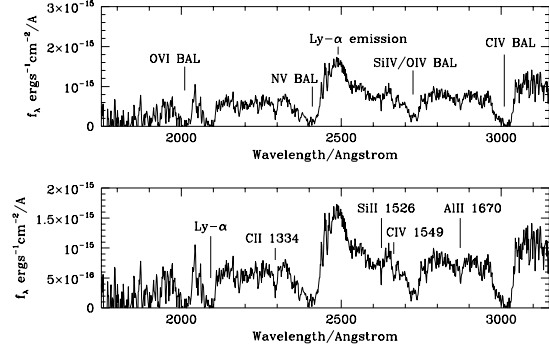


Fig. 4.— The STIS spectrum of FBQS 1137+3907. The upper plot has the quasar Ly $\alpha$  emission (at  $z_Q = 1.02$ ) and BAL features labelled, the lower plot has absorption features associated with the DLA system ( $z_{\text{abs}} = 0.72$ ) labelled.

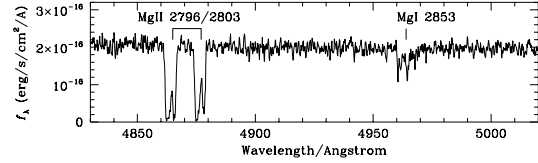


Fig. 5.— The Keck ESI spectrum of FBQS 0051+0041 in the region of the MgII absorption lines.

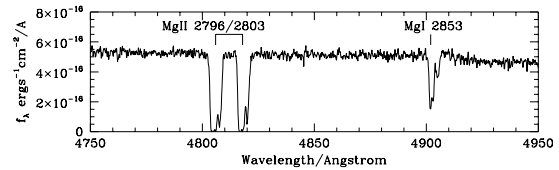


Fig. 6.— The Keck ESI spectrum of FBQS 1137+3907 in the region of the MgII absorption lines.

and 6, and the LRIS spectra of the galaxies at the absorber redshifts in Figures 7 and 8.

### 5. The absorber of FBQS 0051+0041

The *HST* spectrum shows that this absorber is a borderline DLA, with a column density just above the division between Lyman-limit and DLA systems (Table 3). Similarly, the  $EW_0$  of the FeII absorption only just satisfies our selection criteria.

The candidate absorber galaxy, galaxy ‘a’ in Figure 1, seems, at first sight, to be a fairly normal, star forming galaxy, offset by 24kpc from the quasar (Figures 1 and 7). The spectrum, however, shows a small mis-match between the [OII]3727 redshift of 0.740 and the absorption line redshift from the Ca II H+K lines (0.738), though the signal-to-noise ratio of the absorption lines is low. Two distinct velocity components are also seen in the low-ionization MgII, MgI and FeII quasar absorption lines in our ESI spectrum, one at  $z = 0.7393$  and one at  $z = 0.7402$  (i.e. a  $160\text{kms}^{-1}$  velocity difference). Whether these two components correspond to two galaxies, the candidate and a dwarf companion nearer the quasar, or reflect internal gas motions in the candidate absorber is unclear.

### 6. The absorber of FBQS 1137+3907

This is a much higher column density absorber than that of FBQS 0051+0041. The *HST* spectrum shows several strong UV metal absorption lines in addition to the damped Ly $\alpha$  line (Figure 4).

The LRIS slit was placed to cover both candidate absorbing galaxies, *a* and *c*, and line emission is seen from both of them (barely resolved from each other) at the wavelength corresponding to [OII] 3727 at  $z = 0.7185 \pm 0.0003$  (Figure 9). There is also a marginal detection of H $\beta$  at the same redshift (Figure 8). Although we see no other features from *a* or *c*, it seems unlikely that the strong emission line can be anything other than [OII] at the absorber redshift, given its high equivalent width and the lack of lines nearby in the spectrum. We also took a spectrum with the slit aligned with object ‘b’. This showed that ‘b’ had blue optical continuum emission, but no strong features from which to obtain a redshift. As it is further from the quasar than ‘c’ and has no features at wave-

lengths corresponding to the absorption redshift we assume that it is unrelated to the DLA system.

Table 1: Imaging of the FBQS DLA fields

| Quasar field   | Telescope/Instrument | Filter | Observation date (UT) | Total integration time (minutes) | Seeing (arcsec) |
|----------------|----------------------|--------|-----------------------|----------------------------------|-----------------|
| FBQS 0051+0041 | Keck-II/ESI          | $I$    | 2001 June 22          | 20                               | 0.8             |
| FBQS 1137+3907 | Keck-I/NIRC          | $K'$   | 2002 May 25           | 27                               | 0.4             |

Table 2: Observed properties and spectroscopic observations of the FBQS DLA galaxies

| Quasar field    | $z_{\text{gal}}$ | Mag.        | Impact parameter (arcsec) | Impact parameter (kpc) | Abs. mag.     | $\Delta M_k$ | $L/L^*$ | UT Date (deg) | Slit PA | Exposure time (s) |
|-----------------|------------------|-------------|---------------------------|------------------------|---------------|--------------|---------|---------------|---------|-------------------|
| FBQS 0051+0041a | 0.740            | $I = 22.0$  | 3.3                       | 24                     | $M_B = -20.0$ | -0.11        | 0.8     | 2001 Sept 25  | 26      | $2 \times 1200$   |
| FBQS 0051+0041b | ?                | $I = 23.3$  | 4.6                       | ?                      | -             | -            | -       | -             | -       | -                 |
| FBQS 0051+0041c | 0.070            | $I = 23.2$  | 7.2                       | 9.6                    | $M_R = -13.9$ | -0.15        | 0.001   | 2001 Sept 25  | 26      | $2 \times 1200$   |
| FBQS 1137+3907a | 0.7185           | $K' = 19.5$ | 2.5                       | 18                     | $M_K = -23.0$ | -0.08        | 0.3     | 2002 Dec 31   | 126     | $2 \times 1800$   |
| FBQS 1137+3907b | ?                | $K' = 20.4$ | 1.8                       | ?                      | -             | -            | -       | 2002 Dec 31   | 228     | $2 \times 1800$   |
| FBQS 1137+3907c | 0.7185           | $K' = 19.8$ | 1.5                       | 11                     | $M_K = -22.8$ | -0.08        | 0.2     | 2002 Dec 31   | 126     | $2 \times 1800$   |

Notes:  $\Delta M_k$  is the amount that was added to the absolute magnitudes to account for the difference in the flux density of the galaxy between the observed band and the band the absolute magnitude was calculated in. This correction depends only on the assumed galaxy SED and reduces to the usual  $k$ -correction when the two bands are the same.

Table 3: Details of the DLA systems

| Quasar         | $z_{\text{abs}}$ | MgII $EW_0$ (2796) | FeII $EW_0$ (2600) | $\lg(N_{\text{HI}} (\text{cm}^2))$ |
|----------------|------------------|--------------------|--------------------|------------------------------------|
| FBQS 0051+0041 | 0.740            | 2.4                | 1.0                | $20.4 \pm 0.1$                     |
| FBQS 1137+3907 | 0.719            | 3.0                | 2.5                | $21.1 \pm 0.1$                     |

Table 4: Physical properties of galaxies with spectroscopic redshifts consistent with  $z_{\text{abs}}$ 

| Absorber candidate         | $z_{\text{gal}}$ | $\lg(N_{\text{HI}} (\text{cm}^2))$ | Impact parameter (kpc) | Observed mag.    | Absolute mag. | $\Delta M_k$ | $L/L^*$ | Type                | Refs. |
|----------------------------|------------------|------------------------------------|------------------------|------------------|---------------|--------------|---------|---------------------|-------|
| SBS 1543+5921              | 0.009            | 20.4                               | 0.4                    | $R = 16.3$       | $M_R = -16.7$ | -            | 0.02    | LSBG                | 9,10  |
| OI 363 (B0738+313) G1      | 0.221            | 20.9                               | 20                     | $R = 20.8$       | $M_R = -19.4$ | 0.2          | 0.2     | dE                  | 3,4   |
| FBQS 1137+3907c            | 0.720            | 21.1                               | 11                     | $K' = 19.8$      | $M_K = -22.8$ | -0.1         | 0.2     | spiral?             | 1     |
| PKS 1127-145               | 0.312            | 21.7                               | $< 7$                  | $R = 21.6^c$     | $M_B = -19.3$ | -0.2         | 0.4     | LSBG                | 7,8   |
| PKS 1243-072A              | 0.437            | $\approx 20.5^b$                   | 12                     | $I = 21.3$       | $M_R = -20.1$ | 0.2          | 0.4     | starburst/Seyfert 2 | 8     |
| FBQS 0051+0041a            | 0.740            | 20.4                               | 24                     | $I = 22.0$       | $M_B = -20.0$ | -0.11        | 0.8     | spiral?             | 1     |
| B2 0827+243 G1             | 0.526            | 20.3                               | 36                     | $I = 20.3$       | $M_R = -21.6$ | 0.2          | 1.6     | spiral              | 5,6   |
| AO 0235+164 A <sup>a</sup> | 0.524            | 21.7 <sup>b</sup>                  | 13                     | $m_{785} > 20.3$ | $M_R > -22.6$ | 0.3          | $< 4$   | Seyfert 1           | 2     |

Notes: <sup>a</sup> object A1 in ref. 2 is closer to the quasar but has no spectrum, if it is at the absorber redshift it has  $(L/L^*)_B = 1.0$ , A has a bright nuclear component, and the luminosity of the underlying galaxy is uncertain; we have quoted upper limits based on the sum of the host and AGN fluxes. <sup>b</sup> column density from 21cm line absorption, dependent on the assumed spin temperature. <sup>c</sup> sum of components 1-4 of Rao et al. (2003). See Table 3 for the definition of  $\Delta M_k$ . References: (1) this paper; (2) Burbidge et al. 1996; (3) Turnshek et al. 2001; (4) Cohen 2001; (5) Steidel et al. 2002; (6) Rao et al. 2003; (7) Lane et al. 1998; (8) Kanekar et al. 2002; (9) Reimers & Hagen 1998; (10) Bowen et al. 2001

The ESI spectrum shows a complicated velocity profile, with two to four distinct low-ionization absorption components seen, depending on which line is examined. The two deepest features, visible in all the lines, are at  $z = 0.7184$  and  $z = 0.7193$  (i.e. a  $160\text{km s}^{-1}$  velocity difference). Thus the [OII] emission is most likely to be associated with the deeper, less redshifted absorption component.

## 7. Discussion

The DLA absorber candidate close to FBQS 0051+0041 has a luminosity of approximately  $L^*$ , whereas that associated with FBQS 1137+3907 is about  $0.2L^*$ . The galaxy types are unclear. Both are apparently forming stars, possessing both blue continua and [OII] emission lines, and the complicated velocity structures of the MgII absorption lines seen in the ESI spectra, might be indicative of starburst-induced winds (e.g. Ellison et al. 2003). Further evidence for this is the offset between the emission and absorption redshifts in FBQS 0051+0041a, if real. Thus there is some evidence that both may be starburst galaxies. However, the continuum slope of FBQS 0051+0041a is a little too red unless the starburst is reddened by dust, and FBQS 1137+3907c has a high axial ratio, suggesting a spiral rather than an irregular galaxy (though the shape of ‘c’ may also be due to it being composed of a chain of knots). Higher spatial resolution multicolor imaging will be required to determine the nature of these galaxies.

Table 4 summarizes the properties of the eight known candidate DLA galaxies at  $z < 1$  which spectroscopy has shown to lie at the absorber redshift. Selection effects will mean that the absorber population for which spectroscopic identification is possible will be biased. Observational requirements for successful spectroscopy, namely an impact parameter  $\gtrsim 1$  arcsec and an apparent mag-

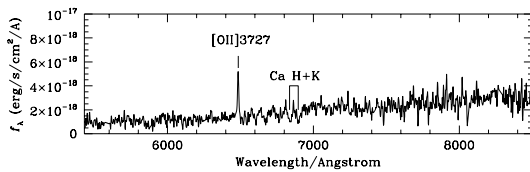


Fig. 7.— The spectrum of galaxy ‘a’ ( $z = 0.740$ ) near FBQS 0051+0041.

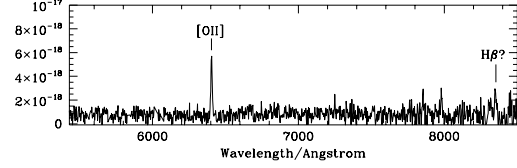


Fig. 8.— The sum of the extracted spectra of galaxies ‘a’ and ‘c’ near FBQS 1137+3907.

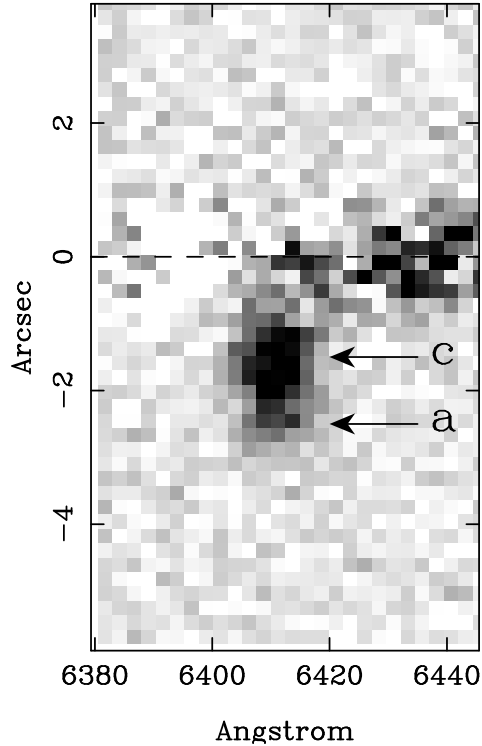


Fig. 9.— The 2D spectrum of galaxies ‘a’ and ‘c’ near FBQS 1137+3907 in the region of the [OII] emission line in the galaxies. The trace of the quasar was averaged for 30 pixels either side of the region shown and the mean subtracted from this portion of the image. The center of the unsubtracted quasar trace is indicated by the dashed line at 0 arcsec. The seeing FWHM was  $0''.92$  (4.3 pixels), so ‘a’ and ‘c’ are only marginally resolved.

nitude brighter than  $R \sim 24$ , will naturally favor massive galaxies. For our FBQS sample discussed in the introduction, and from which FBQS 0051+0041 and FBQS 1137+3907 were drawn, we have so far only successfully identified candidates and obtained spectra with redshifts consistent with those of the absorber system for four out of thirteen of our high  $EW_0$  absorption systems. In addition, there is another subtle selection effect from the way most (though not all) of the DLAs in Table 4 have been selected, namely on the basis of high  $EW_0$  metal absorption lines. This will tend to bias the sample towards higher metallicity, more massive, galaxies. Working against these two effects is the possibility that many of the more massive DLA galaxies are dusty enough to significantly extinguish the light from the background quasar, and cause the quasar to drop out of optically-selected samples. This may tend to produce a bias towards relatively dust-free, less massive hosts, and may explain why the MgII absorbers, with their generally higher impact parameters and lower HI column densities, are observed to have luminosities around  $L^*$ . However, the results of the survey of radio-loud quasars of Ellison et al. (2001) suggest that this is not an important effect. Any such effect will also be much reduced for FBQS quasars as they are selected on the Palomar  $E$ -plates with a relatively red ( $O - E \sim B - R < 2.0$ ) color selection criterion. Thus, despite most of the selection effects favouring successful spectroscopic identification of the most luminous absorbing DLA galaxies, it is clear from Table 4 that many are sub- $L^*$ , and this suggests that the majority of the DLA population is probably sub- $L^*$ .

Both our DLA candidates appear to be actively forming stars, consistent with them being relatively gas-rich galaxies. A large fraction of the known spectroscopically-confirmed DLA systems at low redshift listed in Table 4 appear to be merging or interacting in some way, for example, FBQS 1137+3907c, PKS 1127-145 and PKS 1243-072 A (though obviously the statistics are poor at present, and few apparent pairs have been spectroscopically confirmed). This is intriguing in the light of theories in which DLA galaxies are dwarf galaxies which merge to become massive galaxies today (Haehnelt et al. 1998; Maller et al. 2001). Though these theories are more applicable to the

high redshift systems, the lower redshift DLAs may represent the tail end of this activity.

We thank an anonymous referee for helpful comments. This work was partly carried out at the Jet Propulsion Laboratory, California Institute of Technology, under contract with the National Aeronautics and Space Administration (NASA), and partly under the auspices of the U.S. Department of Energy, National Nuclear Security Administration by the University of California, LLNL, under contract No. W-7405-Eng-48, with additional support from NASA grant HST-GO-09051.01-A and NSF grant AST-00-98355 (University of California, Davis). Some of the data presented herein were obtained at the W.M. Keck Observatory, which is operated as a scientific partnership among the California Institute of Technology, the University of California and NASA. The observatory was made possible by the generous financial support of the W.M. Keck Foundation. The authors wish to acknowledge the significant cultural role and reverence that the summit of Mauna Kea has always had within the indigenous Hawaiian community. This research has also made use of the NASA/IPAC Extragalactic Database (NED) which is operated by the Jet Propulsion Laboratory, California Institute of Technology, under contract with NASA.

## REFERENCES

- Becker, R.H. et al. 2001, ApJS, 135, 227
- Bergeron, J. & Stasińska, G. 1986, A&A, 169, 1
- Boisse, P., Le Brun, V., Bergeron, J. & Deharveng, J.-M. 1998, A&A, 333, 841
- Boissier, S., Peroux, C. & Pettini, M. 2003, MNRAS, 338, 131
- Bowen, D.V., Tripp, T.M. & Jenkins, E.B. 2001, ApJ, 121, 1456
- Burbidge, E.M., Beaver, E.A., Cohen R.D., Junkkarinen, V.T. & Lyons, R.W. 1996, AJ, 112, 2533
- Cohen, J.G. 2001, AJ, 121, 1275
- Efstathiou, G. 2000, MNRAS, 317, 697



- Ellison, S.L., Yan, L., Hook, I.M., Pettini, M., Wall, J.V. & Shaver, P. 2001, *A&A*, 379, 393
- Ellison, S.L., Mallén-Ornelas, G. & Sawicki, M. 2003, *ApJ*, in press (astro-ph/0302147)
- Haehnelt, M.G., Steinmetz, M. & Rauch, M. 1998, *ApJ*, 495, 647
- Kanekar, N., Athreya, R.M. & Chengalur, J.N., 2002, *A&A*, 382, 838
- Kulkarni, V., et al. 2001, *ApJ*, 551, 37
- Landolt, A.U. 1992, *AJ*, 104, 340
- Lane, W., Smette, A., Briggs, F., Rao, S., Turnshek, D. & Meylan, G., 1998, *AJ*, 116, 26
- Le Brun, V., Bergeron, J., Boissé, P. & Deharveng, J.M. 1997, *A&A*, 321, 733
- Lin, H., Kirshner, R.P., Shethman, S.A., Landy, S.D., Oemler, A., Tucker, D.L. & Schechter, P.L. 1996, *ApJ*, 464, 60
- Loveday, J. 2000, *MNRAS*, 312, 557
- Maller A.H., Prochaska, J.X., Somerville, R.S. & Primak, J.R. 2001, *MNRAS*, 326, 1475
- Norberg, P., et al. 2002, *MNRAS*, 336, 907
- Persson, S.E., Murphey, D.C., Krezeminski, W., Roth, M. & Rieke, M.J. 1998, *AJ*, 116, 2475
- Pettini, M., Ellison, S.L., Steidel, C.C. & Bowen, D.V. 1999, *ApJ*, 510, 576
- Prochaska, J.X. & Wolfe, A.M. 1998, *ApJ*, 507, 113
- Rao, S. & Turnshek, D.A. 2000, *ApJS*, 130, 1
- Rao, S., Nestor, D.B., Turnshek, D.A., Lane, W.M., Monier, E.M. & Bergeron, J. *ApJ*, submitted (astro-ph/0211297)
- Ridgway, S.E. & Stockton, A.N. 1997, *AJ*, 114, 511
- Rocca-Volmerange, B. & Fioc, M. 1997, *A&A*, 326, 950
- Reimers, D. & Hagen, H.-J. 1998, *A&A*, 329, L25
- Stanford, S.A., Eisenhardt, P.R.M. & Dickinson, M. 1995, *ApJ*, 450, 512
- Steidel, C., Dickinson, M. & Persson, E. 1994, *ApJ*, 437, L75
- Steidel, C., Kollmeier, J.A., Shapley, A., Churchill, C.W., Dickinson, M. & Pettini, M. 2002, *ApJ*, 570, 526
- Songaila A., Cowie L.L., Hu E.M., Gardner J.P., 1994, *ApJS*, 94, 461
- Storrie-Lombardi, L.J, McMahon, R.G., Irwin, M.J. & Hazard, C. 1996, *ApJ*, 468, 121
- Storrie-Lombardi, L.J. & Wolfe, A.M. 2000, *ApJ*, 543, 552
- Turnshek D.A., Rao, S., Nestor, D., Lane, W., Monier, E., Bergeron, J. & Smette, A. 2001, *ApJ*, 553, 288
- Warren, S.J., Moller, P., Fall, S.M. & Jakobsen, P. 2001, *MNRAS*, 326, 759
- White, R.L. et al. 2000, *ApJS*, 126, 133
- Zwaan M., Briggs, F.H. & Verheijen, M. 2002, in *Extragalactic Gas at Low Redshift*, eds J.S. Mulchaey & J. Stocke, ASP Vol. 254, p. 169